an acceptable match between the observed and the calculated anomalies is obtained. The FIT-3D[17] software for performing this inversion was used. The basement picture (Figure 3) thus evolved provides a synoptic view of major basement domains and associated structural features. It is a clear representation of the Papaghni sub-basin. This shows a bulging in the southwestern part of the basin, more or less coinciding with the boundary of the Cuddapah Basin in the south and southwestern part of the basin. The basement attains a maximum depth of about 10 km near Muddanuru.

The central depression in basement is observed to be elongated in NW-SE direction with steep dips in the southern and southwestern sides, suggesting that the sediment filling the depression was derived from the southern and southwestern side of the basin. An east-west elongation was observed over a part of the depression (clearly seen in contour pattern) nearly along and below 15°N parallel and above Tadipatri, where the Kunder river followed the same direction and thereafter took a turn towards the basin centre. And in the northern side, the depression boundary is truncated in E-W direction, which might be the representation of the E-W Banganpalle Fault. The basement high further north to the Banganpalle Fault may be a transition zone between Papaghni Basin and the northern Kurnool sub-basin. It seems from this basement map that the western sub-basin is bounded by faults in the north and the southwest directions. The maximum thickness of the sediment in this area is observed to be about 10 km near Muddanuru.

A part of the Kavali–Udupi Deep Seismic Sounding (DSS) survey carried out by NGRI[14,15] reveals the structure and tectonics of the south Indian peninsula along this profile. A part of this profile passes through the present study area and the basement depths inferred from the DSS are comparable to those obtained in the present analysis.

It may be mentioned here that the basement picture derived by pseudo-gravity transformation of aeromagnetic data is based on the assumption that the magnetization is solely by induction. If remanance is present in any other direction than the present field, then the picture will be different. However, as the results of the present analysis are in general agreement with the geological understanding and other geophysical information such as DSS, the basement picture provided here may be considered to present a qualitative description of the basement in this part of the area.

1. King, W., *Geol. Surv. India, Mem.*, 1872, 8, 346.
2. Murthy, Y. G. K., 4th Workshop on Status, Problems and Programmes in Cuddapah Basin, Institute of Indian Peninsular Geology, Hyderabad, 1982, pp. 51–72.
3. Nagaraja Rao, B. K., Rajurkar, S. T., Ramalingaswamy, G. and Ravindra Babu, B., *Geol. Soc. India, Mem.*, 1987, 6, 33–86.
4. Narayanaswamy, S., *J. Geol. Soc. India*, 1966, **7**, 33–50.
5. Atchuta Rao, D., Sankernarayan, P. V. and Harinarain, *Bull. Natl. Geophys. Res. Inst.*, 1970, **8**, 129–151.
6. Babu Rao, V., Atchuta Rao, D., Rama Rao, Ch., Sarma, B. S. P., Bhaskara Rao, D. S., Veeraswamy, K. and Sarma, M. R. L., *Geol. Soc. India, Mem.*, 1987, **6**, 295–312.
7. Mishra, D. C., Babu Rao, V., Laxman, G., Rao, M. B. S. V. and Venkatarayadu, M., *Geol. Soc. India, Mem.*, 1987, 6, 313–330.
8. Balakrishna, S., Christopher, G. and Ramana Rao, A. V., Proceedings of the Symposium on Upper Mantle Project, NGRI Publ., 1967, vol. 8, pp. 303–319.
9. Kailasam, L. N., *Tectonophysics*, 1976, **76**, 225–245.
10. Krishna Brahmam, N., *J. Geol. Soc. India*, 1989, **34**, 373–384.
11. Qureshy, M. N., Krishna Brahmam, N. Aravamadhu, P. S. and Naqui, S. M., *Proc. R. Soc. London, Ser. A*, 1968, **304**, 449–464.
12. Ram Babu, H. V., *Tectonophysics*, 1993, **223**, 411–422.
13. Verma, R. K. and Satyanarayana, A., *ibid*, 1990, **178**, 337–356.
14. Kaila, K. L. and Tewari, H. C., *ibid*, 1985, **115**, 69–86.
15. Kaila, K. L. *et al.*, *J. Geol. Soc. India*, 1979, **20**, 307–333.
16. GEOSOFT, Software for air-borne data processing, Toronto, Canada.
17. FIT-3D, Software for gravity and magnetic data modelling, Paterson Grant and Watson, Toronto, Canada.

ACKNOWLEDGEMENTS. We are grateful to the Director, NGRI for permission to publish this work.

Received 22 November 2001; revised accepted 4 March 2002

Variations in nearshore processes along Nagapattinam coast, India

V. Sanil Kumar*, N. M. Anand and R. Gowthaman

Ocean Engineering Division, National Institute of Oceanography, Dona Paula, Goa 403 004, India

Directional wave data collected at 10 m water depth, at 2 km distance off Nagore from March 1998 to February 1999, were used to estimate the longshore currents and longshore sediment transport rate considering the sea and swell waves separately using the CERC formula. Daily littoral environmental parameters were observed at three stations and longshore sediment transport rate was estimated using Walton's equation. A comparative study was carried out on theoretical and measured longshore currents. The ratio of spectral energy at the first and second spectral peaks shows that energy at the second peak was more than 50% of the energy at the first peak in 43% of the data collected, due to the presence of sea and swell waves. The difference between the sediment transport rate estimated based on the two methods is around 3.5%. The sediment transport using CERC formula shows that average annual gross transport was 0.448×10^6 m^3 and the average annual net transport (towards south) was 0.098×10^6 m^3 and this contributes to the supply of sediment to the Palk Bay.

THE Nagapattinam–Poompuhar coastline (Figure 1) consists of long, narrow and low sandy beaches. The nearshore bathymetry is relatively steep, straight and parallel

*For correspondence. (e-mail: sanil@darya.nio.org)

to the coast. The beach sediments consist of medium to fine sand with considerable placer minerals like garnet and ilmenite. The nearshore seabed consists of fine sand, silt and clay. The tides in this region are semi-diurnal with an average spring range of 0.67 m and neap range of 0.19 m. Extreme wave conditions occur during severe tropical cyclones which are frequent in the Bay of Bengal during the northeast monsoon (October to January). The presence of shallow Palk Bay and Sri Lanka island significantly controls the pattern of longshore transport along the Tamil Nadu coast. The pattern of longshore transport rate has been investigated based on the collected directional wave data for this region[1] and for the South Tamil Nadu coast[2]. Earlier works were mostly based on historical ship reports on waves and dredging records[3,4]. The striking feature of the east coast of India is its large littoral drift, said to be the largest among the world coastlines[3,5–7]. Wave statistics around the Indian coast was studied based on ship-reported, deep-water wave data[8].

The objective of the work was to study the variations in wave climate based on the data collected in two different years, longshore currents and sediment transport along the Nagapattinam coast. To obtain directional wave data,

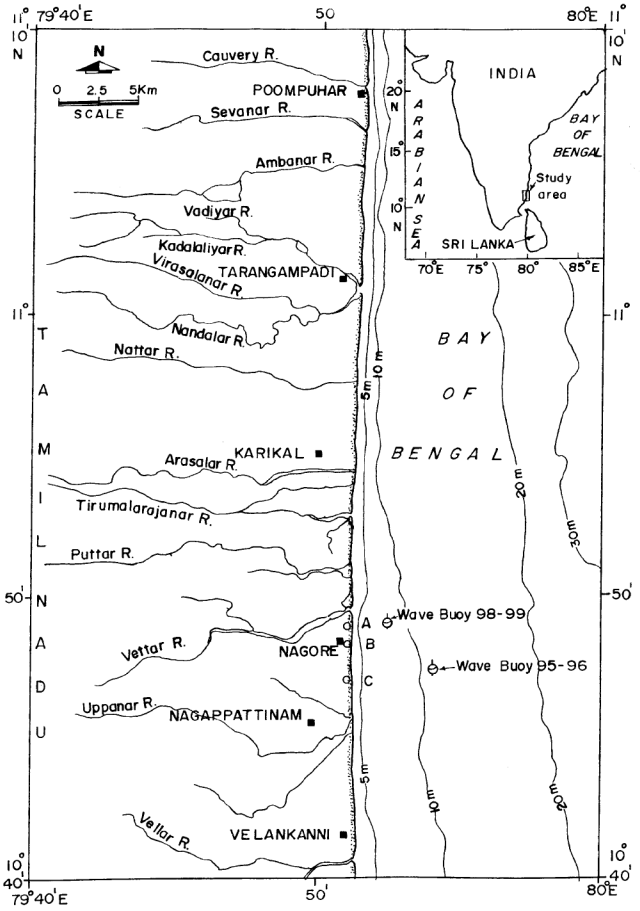

Figure 1. Study area.

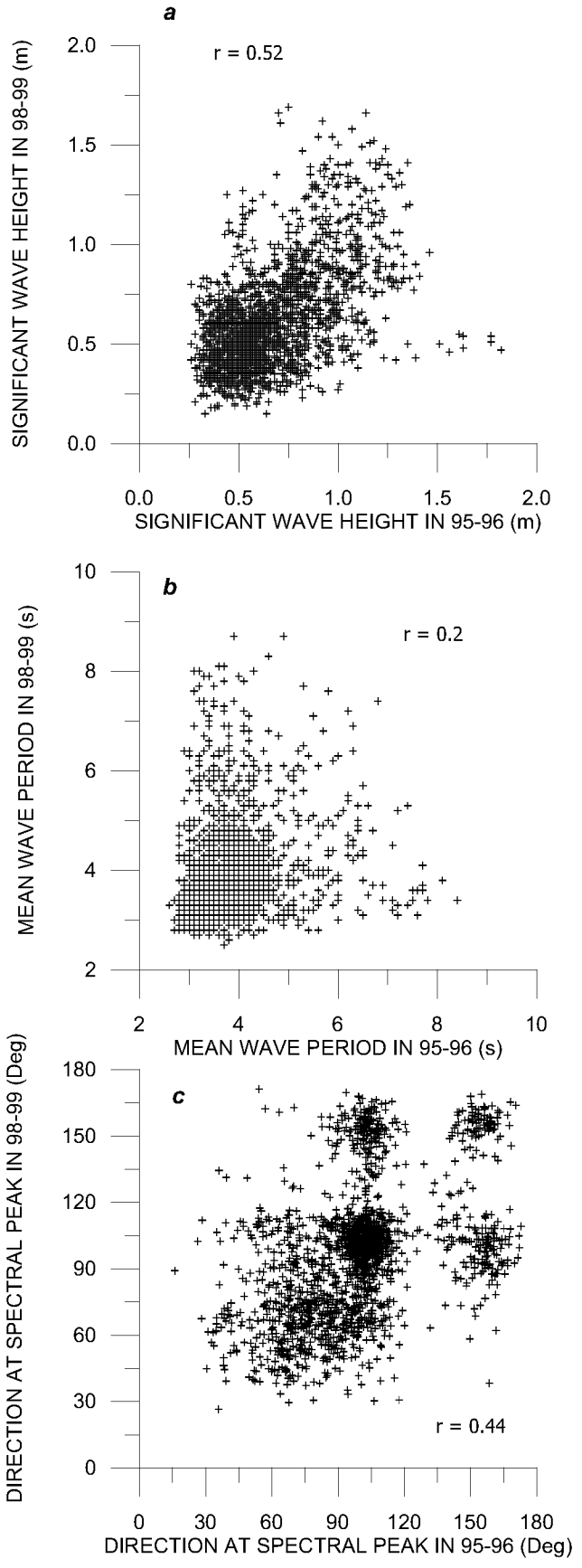

Figure 2. Variation of (*a*) significant wave height, (*b*) mean wave period, and (*c*) wave direction for data sets 1995–96 and 1998–99.

a Datawell directional wave rider buoy was deployed at 10 m water depth, at a distance of 2 km off Nagore. Data were recorded for 20 min duration, at 3 h intervals for a period of one-year (from March 1998 to February 1999) and compared with the data obtained during March 1995 to February 1996 at 15 m water depth, at 5 km distance off Nagapattinam (Figure 1). The distance between the two locations was 4.5 km. Measured waves and the daily littoral environmental parameters[9] observed at three stations were used to estimate the longshore sediment transport rate.

Based on the measured wave data, significant wave height (H_s), mean wave period (T_{02}) and wave directions (with respect to north) corresponding to the primary peak (maximum spectral energy) and secondary peak of the spectrum were estimated[2]. This has become necessary because the wave spectra were mainly double-peaked with contribution from seas and swells. The sea and swell waves were separated as follows. A cut-off frequency was determined between the two peak frequencies, where the spectral energy was minimum and the wave spectrum was divided into two parts. Then the wave height, wave period and wave direction of both wave fields, seas and swells were calculated for each record based on the spectral method.

The wave height and direction of the sea and swell waves measured at 10 m water depth were reduced to wave-breaking zone[10,11]. The wave-shoaling coefficients were estimated using small-amplitude wave theory. The wave directions measured at 10 m water depth were corrected to refraction effects using Snell's law and the breaker angles of sea and swell waves were calculated separately assuming no wave–wave interaction. Hence in the present study two breaker heights and two breaker angles corresponding to the sea and swell waves were estimated.

Visual observation on surf zone width and measurement of longshore currents were carried out daily at three stations, A, B and C (Figure 1) – north of Nagapattinam during March 1998 to February 1999. Magnitude and direction of the longshore currents were measured daily at these stations using Rhodamine-B dye in the surf zone, approximately at one third of the surf zone width distance from the shoreline. The distance covered in 2 min was measured and the average longshore current was estimated.

Two commonly used equations to estimate the longshore current are[12,13]:

$$V_G = K\, g\, m\, T \sin 2\alpha_b, \quad (1)$$

$$V_{LH} = 20.7\, m\, (gH_b)^{1/2} \sin 2\alpha_b, \quad (2)$$

where V_G and V_{LH} are the mean longshore current velocities in the surf zone in m/s, K is a dimensionless coefficient depending solely on the geometry of the breaking wave which is taken as unity[14], g is acceleration due to gravity in m/s^2, m is the foreshore slope, T is the wave period in s, H_b is the breaker height in m and α_b is the breaker angle (angle between the breaking wave crest and the shoreline). The longshore currents were estimated for the sea and swell waves separately and the resultant was estimated as the vectorial sum of both.

The longshore sediment transport rate is usually estimated using CERC formula[15,16] and its suitability to the Indian coast had been already assessed[17]. The computed breaker parameters of sea and swell waves based on the measured wave data were used for estimating the longshore sediment transport using CERC formula. The CERC formulation assumes that all the energy is associated with a single peak in the wave spectra. Comparison of the longshore sediment transport rate computed using CERC formula based on spectral peak wave parameters at breaking and measured values showed that predicted values compared reasonably well, except when the sea and swell directions are different[18]. In the present case, the wave spectrum was double-peaked and hence the wave characteristics of sea and swell waves were considered separately for estimating the longshore sediment transport rate. The daily observed breaker height, surf zone width and the measured longshore current speed were used to estimate the longshore sediment transport using Walton's equation[19]. The friction coefficient was taken as 0.01 (ref. 13).

The significant wave height varied from 0.3 to 1.8 m, with an average value of 0.67 m during 1995–96 and from 0.2 to 1.7 m, with an average value of 0.63 m during 1998–99 (Figure 2 *a*). The highest wave heights were recorded in November. The mean wave period predominantly varied from 3 to 8 s, with an average value of 4 s during both periods (Figure 2 *b*). The wave direction corresponding to the primary spectral peak (with respect to north) mostly prevailed between 60 and 120° during November–February, and 90 and 120° during the rest of the year. The average value of the wave direction was 100° during 1995–96 and 98° during 1998–99 (Figure 2 *c*). The maximum wave height was 1.65 times the significant wave height, with the wave heights following the Rayleigh distribution in both periods (Figure 3 *a* and *c*). Even though the spectra were multi-peaked, the maximum spectral density was estimated reasonably well with Scott spectra[20]. The probable reason is that validation of Scott spectrum was carried out using considerable swell-

Table 1. Range and average value of different parameters

Parameter	Range	Average value
H_s (sea)	0.1–1.3 m	0.5 m
T_{02} (sea)	2.1–6.0	3 s
Wave direction (sea)	15–170°	106°
H_s (swell)	0.1–1.1 m	0.4 m
T_{02} (swell)	6.0–17.6	9 s
Wave direction (swell)	38–168°	99°

dominated data and a similar situation prevails at many sites along the Indian coast. The maximum spectral density estimated from measured data and with that from Scott is shown in Figure 3 *b* and *d*.

Even though the wave measurements were carried out at 15 m and 10 m water depths, the comparison shows that the statistics of the wave parameters was almost the same during both periods, but the events did not occur in the same time for both the years. The wave spectra were single peaked in 31% of the data collected during 1995–96 and 37% in 1998–99. The ratio of spectral energy at the first and second spectral peaks estimated shows that the energy at the second peak is more than 50% of the energy at first peak in 46% of the data collected in 1995–

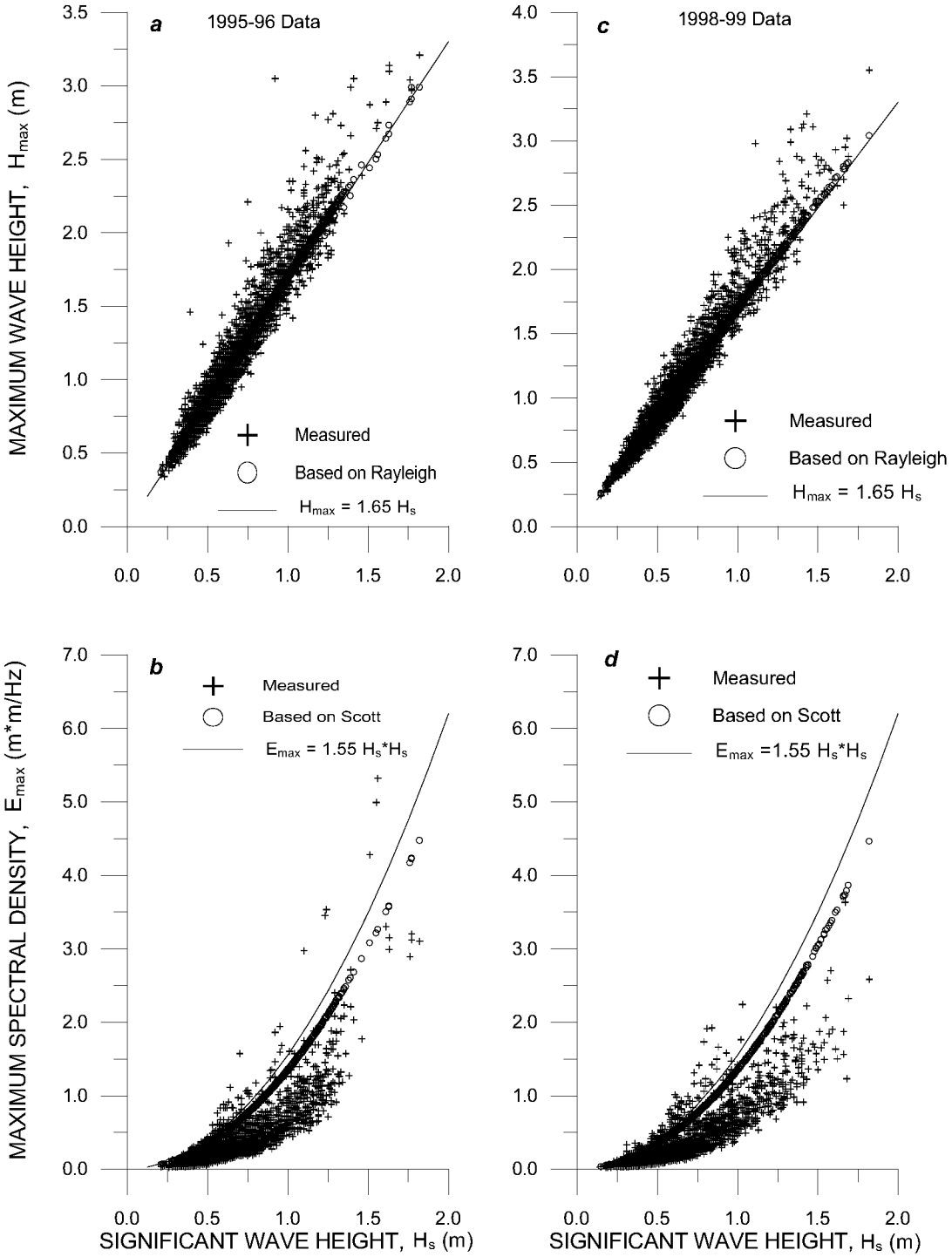

Figure 3. Variation of (*a*) maximum wave height with significant wave height and (*b*) maximum spectral density with significant wave height for 1995–96 data. Variation of (*c*) maximum wave height with significant wave height and (*d*) maximum spectral density with significant wave height for 1998–99 data.

96 and 43% in 1998–99. This is due to the presence of sea and swell waves, hence the directions of sea and swell waves were considered in the estimation of longshore current and sediment transport based on the 1998–99 wave data. The range and the average value of the sea and swell parameters measured during 1998–99 show that the H_s values were similar (Table 1), but the mean wave period and direction were not the same. Hence the wave period and direction of the sea and swell will give rise to difference in longshore current and consequently the sediment transport.

The estimated breaker height is shown in Figure 4 *a*. The estimated breaker angle corresponding to the wave direction of sea and swells is shown in Figure 4 *b*. The

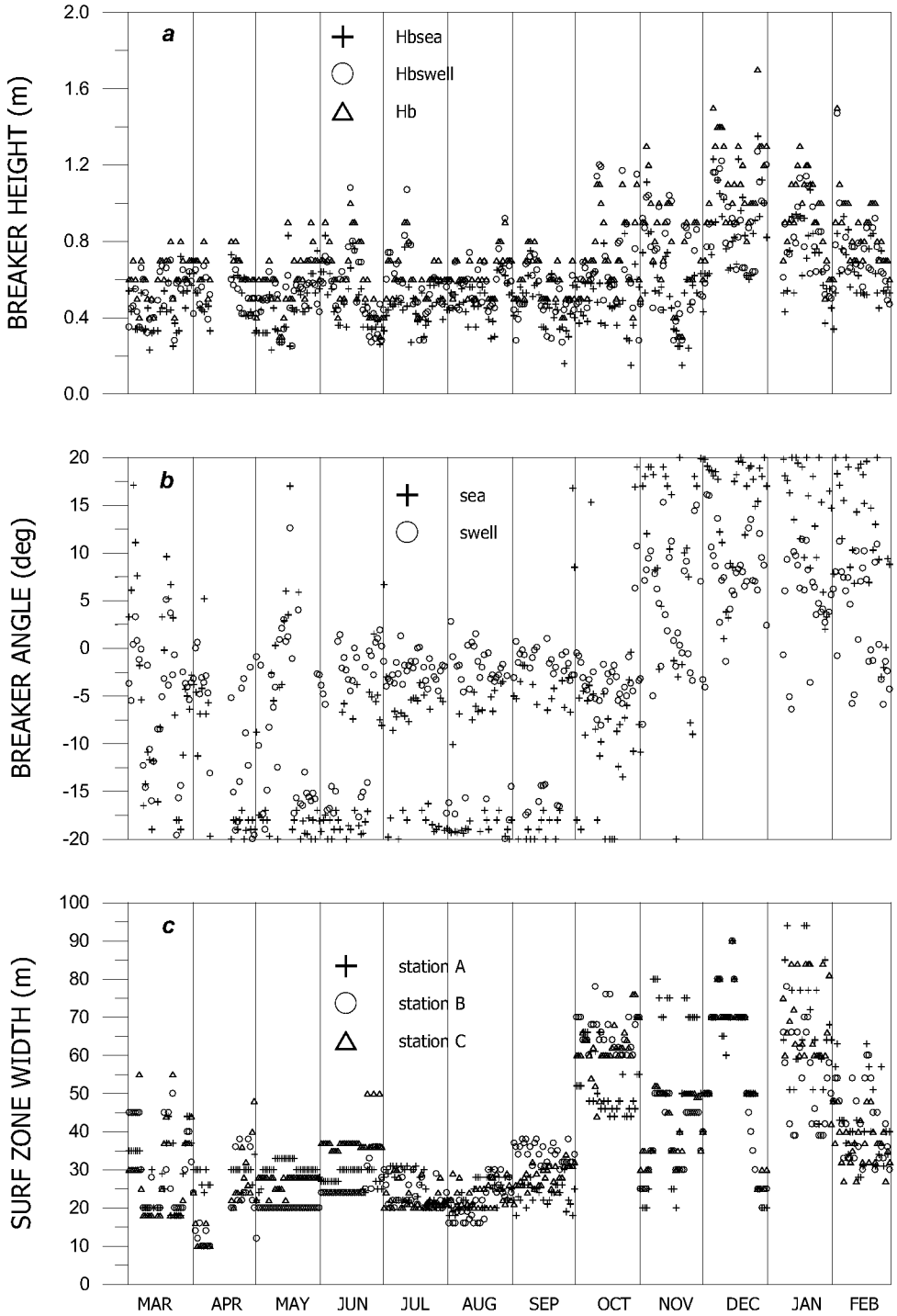

Figure 4. Variation of (*a*) breaker height of sea and swell waves, (*b*) breaker angle with respect to coast of sea and swell waves, and (*c*) surf zone width for stations A, B and C.

breaker angle of waves approaching the coast from the south was considered as negative and that for waves approaching the coast from the north was considered as positive. The average value of the breaker angle for the sea waves was $-3.3°$ and that for the swells was $2°$. Figure 4 shows that breaking sea and swell waves were mainly from the southerly direction during March–October and mainly from the northerly direction during the rest of the year. Breaker angle varied from $-20°$ (during the southwest monsoon period) to $+20°$ (during the northeast monsoon period).

Plunger-type wave breakers were observed in June, November and December, and mostly spilling was found during the rest of the year. The width of the surf zone was larger (> 40 m) during the northeast monsoon period (October to January), between 20 and 60 m during February–March, and between 10 and 40 m during the rest of the year (Figure 4 *c*)). The average value of the surf zone width was around 37 m.

The daily variations of longshore current estimated based on Longuet–Higgins equation (V_L) and Galvin's equation (V_G) with the measured current at three stations are shown in Figure 5. It shows that the average longshore current speed was 0.25 m/s at all stations, and it was predominantly towards north during March–October and towards south during November–February. This matches with the earlier study[1] carried out in the region. During 1998–99, strong longshore currents (> 0.5 m/s) were observed in November and December. Longshore current was relatively weaker (< 0.5 m/s) during the rest of the year. During 1995–96, strong longshore currents (> 0.6 m/s) were noticed in May, June, November and December. Longshore current was relatively weaker (< 0.3 m/s) from January to April. The computed longshore current speed estimated based on Galvin and Longuet–Higgins was about ± 50% of the measured one. The average correlation coefficient between measured and computed data was around 0.75. For the southern Tamil Nadu coast, longshore current speed was estimated reasonably well[2] with Galvin's equation, with a discrepancy of 6.5%.

The average coastal orientation of this coast is N1°W (i.e. 359° clockwise to north). The 3-hourly measured sea and swell characteristics reduced to breaker zone were used and the estimated monthly transport is presented in Table 2. It shows that the annual longshore sediment transport was 0.175×10^6 m^3 in the northerly direction (March to October) and 0.273×10^6 m^3 in the southerly direction (November to February). The annual net sediment transport was 0.098×10^6 m^3 in the southerly direction and the annual gross sediment transport was 0.448×10^6 m^3.

Even though the CERC formula works well without considering the size of the sand[21], a weak grain-size dependence was confirmed based on dimensional analysis, relating sediment transport with root mean square value of breaker height, beach slope at break-point, deep-water wave length corresponding to the peak wave period and median size of sediment[22]. Large variations in grain size of beach materials (sand to gravel and cobble stones) may cause large differences in estimation of longshore sediment transport rate, and if grain sizes are limited to fine and medium sand (0.15 to 0.4 mm) the difference will be small[23]. The beach sediments along the study area consist of medium to fine sand with considerable placer minerals like garnet and ilmenite[24]. This is due to the fact

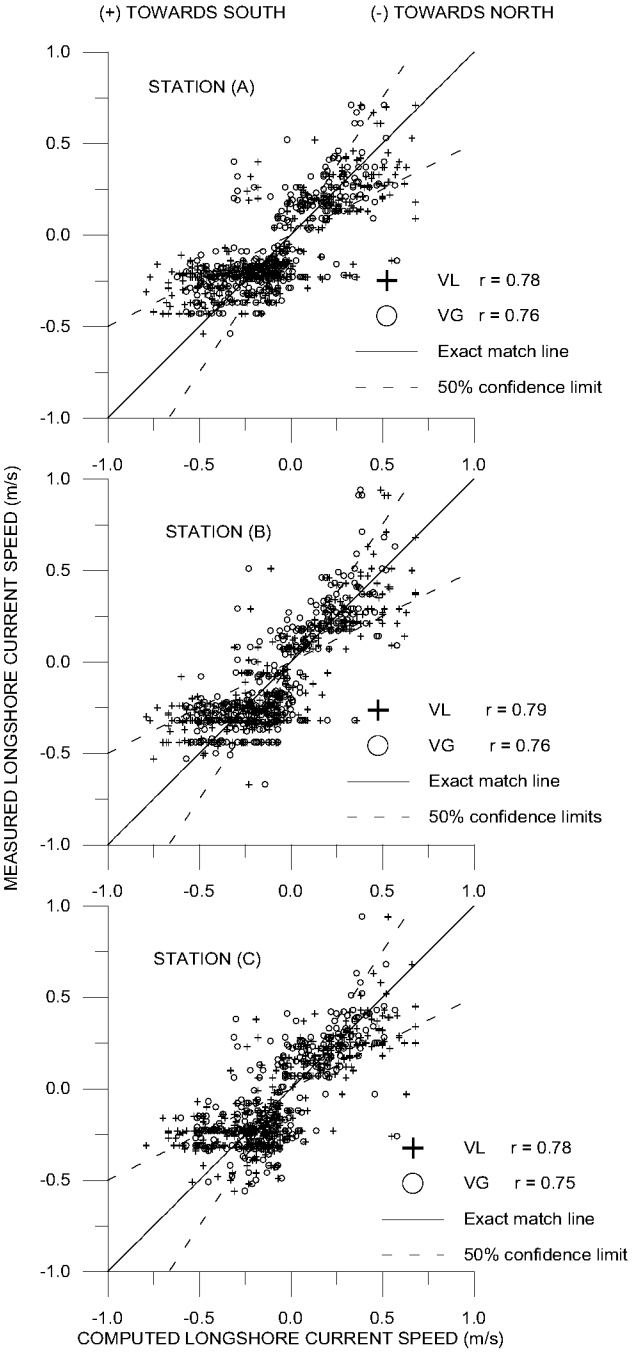

Figure 5. Comparison of longshore current velocity computed based on Longuet–Higgins and on Galvin with the measured current for three stations.

that wave activity along this coast is weak. Particle size is large in coasts subjected to severe wave action and small in coasts subjected to weak wave action[25]. The measurement of total longshore sediment transport rate in the surf zone at a temporary groyne installed at Indian Rocks Beach, west-central Florida showed that the factor 'K', appearing in the CERC formula is not a constant and other factors may enter such as breaker type, turbulence intensity and threshold for sediment transport[26]. The measured total sediment transport rates by the streamer traps and short-term impoundment along the low-wave energy coasts show that the measured values are lower than those predicted by the various empirical formula[27]. Using the root mean square wave height in the CERC formula, the empirical constant value was found to be 0.08 instead of 0.78 recommended in the Shore Protection Manual. In the present study, K was taken as 0.39, with H_s instead of root mean square wave height.

The average longshore current measured in the surf zone was used to estimate the sediment transport using Walton's equation and is presented in Table 3 for stations A to C. Annual longshore sediment transport was 0.168, 0.178 and 0.160×10^6 m^3, respectively, for stations A to C in the northerly direction during March–October. It was 0.264, 0.272 and 0.254×10^6 m^3, respectively, for stations A to C in the southerly direction during November–February. The annual net sediment transport was 0.096, 0.094 and 0.094×10^6 m^3, respectively, at stations A to C in the southerly direction and the annual gross sediment transport was 0.432, 0.450 and 0.414×10^6 m^3, respectively.

The distance between the stations A and B was 1200 m and that between stations B and C was 2200 m. The net sediment transport estimated shows that the movement is towards the south. At station A, the net sediment transport is 0.096×10^6 m^3 and at station B, it is 0.094×10^6 m^3. Hence from stations A to B there is a loss of 2000 m^3 material in the littoral transport system. The beach profile studies carried out up to 1 m below the low tide level[1] show that at station A, erosion was noticed

Table 2. Estimated longshore sediment transport rate in 1000 m^3 based on measured wave data

	Based on sea waves			Based on swell waves			Resultant		
Month	N	S	Net*	N	S	Net*	N	S	Net*
March 1998	6.4	2.3	– 4.1	7.4	1.3	– 6.1	13.4	3.2	– 10.2
April 1998	11.2	0.0	– 11.2	8.4	0.0	– 8.4	19.5	0.0	– 19.5
May 1998	12.7	0.8	– 11.9	10.6	0.7	– 9.9	23.2	1.4	– 21.8
June 1998	17.6	0.0	– 17.6	16.0	0.0	– 16.0	33.5	0.0	– 33.5
July 1998	13.2	0.0	– 13.2	7.8	0.0	– 7.8	21.0	0.0	– 21.0
August 1998	15.3	0.0	– 15.3	7.9	0.1	– 7.8	23.0	0.0	– 23.0
September 1998	11.3	0.2	– 11.1	8.3	0.0	– 8.3	19.4	0.0	– 19.4
October 1998	10.9	3.1	– 7.8	25.2	6.7	– 18.5	36.1	9.8	– 26.3
November 1998	0.8	25.2	24.4	1.5	21.2	19.7	1.9	46.1	44.2
December 1998	0.0	64.8	64.8	0.2	54.6	54.4	0.0	119.2	119.2
January 1999	0.0	46.8	46.8	0.8	27.7	26.9	0.0	73.7	73.7
February 1999	0.1	24.2	24.1	2.4	14.7	12.3	0.8	37.1	36.3
Annual net transport			68.0			30.0			98.0
Annual gross transport			252.0			196.0			448.0

*(–), Northerly transport (N); (+), Southerly transport (S).

Table 3. Estimated longshore sediment transport rate in 1000 m^3 based on Walton's equation

	Station A			Station B			Station C		
Month	N	S	Net*	N	S	Net*	N	S	Net*
March 1998	12.0	1.7	– 10.3	13.6	3.4	– 10.2	12.2	2.2	– 10.0
April 1998	17.0	0.0	– 17.0	18.8	0.0	– 18.8	19.5	0.0	– 19.5
May 1998	21.5	0.0	– 21.5	19.9	0.0	– 19.9	19.3	0.0	– 19.3
June 1998	33.0	0.0	– 33.0	32.8	0.0	– 32.8	33.6	0.0	– 33.6
July 1998	21.9	0.0	– 21.9	21.6	0.0	– 21.6	17.5	0.0	– 17.5
August 1998	23.2	0.0	– 23.2	23.0	0.0	– 23.0	21.8	0.0	– 21.8
September 1998	15.6	1.3	– 14.3	25.8	0.9	– 24.9	18.1	2.6	– 15.5
October 1998	37.1	10.0	– 27.1	45.1	18.6	– 26.6	39.1	16.4	– 22.7
November 1998	6.6	52.0	45.4	3.2	46.8	43.5	5.4	52.1	46.7
December 1998	4.9	114.7	109.9	3.4	122.4	119.0	1.3	97.4	96.1
January 1999	0.0	73.4	73.4	0	73.0	73.0	0.0	76.1	76.1
February 1999	0.0	35.8	35.8	0	36.1	36.1	0.0	35.2	35.2
Annual net transport			96.0			94.0			94.0
Annual gross transport			433.0			449.0			414.0

*(–), Northerly transport (N); (+), Southerly transport (S).

during April–June and October, and the beach was building up from November. There was no net change at the beach in an annual cycle, which shows that part of the change in the transport rate may be due to the onshore–offshore transport of the materials, and which is not studied in this case. From stations B to C there was not much change in the net transport.

The study shows that the average annual net sediment transport was 0.095×10^6 m^3 in the southerly direction and average annual gross sediment transport was 0.432×10^6 m^3. The net sediment transport is towards the south, since the wave activity is strong mainly during the northeast monsoon period for this coast. The annual net sediment transport computed using the estimated breaker angle gives a value of 0.098×10^6 m^3 and the difference between the estimated sediment transport rates based on the two methods is around 3.5%. This is due to error in observation of the surf zone width, which is based on visual observation. Also the wave–wave and the wave–current interactions in the surf zone are not considered. Hence the sediment transport rates estimated based on CERC formula using the measured wave characteristics can be taken as the representative value for this coast.

An earlier study[1] shows that transport rate was around 0.1×10^6 m^3/month in November and December, and was low ($< 0.03 \times 10^6$ m^3/month) in March, April and July. The predominant direction of transport is northerly from March to October and southerly from November to February. Though the annual gross transport was found to be 0.6×10^6 m^3/year, the annual net transport was very low showing less than 0.006×10^6 m^3/year (towards the north). The difference in longshore sediment transport rates between the present study and the earlier study was that in the present study the wave direction of the sea and swell waves was considered in estimation, whereas it was neglected in the earlier study. The energy at the second peak was more than 50% of that at first peak in 46% of the data collected. The coastal inclination of the study area is 359° with respect to north. A wave direction more than 89° will cause a northerly sediment transport and one less than 89° will cause a southerly transport. The average direction of sea waves was 106° and that of the swell waves was 99°. Hence a small error of the order of 0.5° in the estimate of the breaker angle may cause a change in direction of the sediment transport rate. The error in wave directions can lead even to a wrong direction for the net calculated sediment transport[28]. The present alignment of the coastline is found to be sensitively balanced, since any slight increase in approaching wave angles may significantly increase the volume and may also alter the direction of sediment transport in this region. For a coastal inclination of 4° with respect to the north (5° more than the present alignment), the net sediment transport increases to 1.85 times the present value, and for 354° (5° less than the present alignment) the value reduces to 0.12 times the present value.

It is important to notice that no cyclone had occurred during both the study periods, which is otherwise common during the northeast monsoon period. It has been observed that for the occurrence of every cyclone, there was a permanent loss of beach due to erosion[1]. As the Palk Bay is well protected for southerly waves, no mechanism is set to transport these deposited materials towards the north.

The comparison of the wave data collected during 1995–96 and those collected during 1998–99 shows that the statistics of the wave parameters was almost the same during both the periods, but the events did not occur at the same time. The average value of the breaker angle for the sea waves was – 3.3° and that for the swells was 2°; the breaking sea and swell waves were mainly from the southerly direction during March–October and mainly from the northerly direction during the rest of the year. The ratio of spectral energy at the first and second spectral peaks estimated shows that the energy at the second peak is more than 50% of that at first peak in 46% of the data collected in 1995–96 and 43% collected in 1998–99. The daily longshore currents measured show that the average longshore current speed was 0.25 m/s; the longshore current was predominantly towards the north during March–October and towards the south during the rest of the year. The difference between the estimated sediment transport rates based on the two methods is around 3.5%. This is due to the error in observation of the surf zone width. The annual net sediment transport was 0.098×10^6 m^3 in the southerly direction and annual gross sediment transport was 0.448×10^6 m^3, and this contributes to the supply of sediment to the Palk Bay.

1. Jena, B. K., Chandramohan, P. and Sanil Kumar, V., *J. Coast. Res.*, 2001, **17**, 322–327.
2. Sanil Kumar, V., Chandramohan, P., Ashok Kumar, K., Gowthaman, R. and Pednekar, P., *ibid*, 2000, **16**, 247–254.
3. Saxena, P. C., Vaidyaraman, P. P. and Srinivasan, R., *Proc. Coast. Eng.*, 1976, **2**, 1377–1393.
4. Chandramohan, P., Nayak, B. U. and Raju, V. S., *J. Waterway, Port, Coast. Ocean Eng.*, 1990, **116**, 408–423.
5. Komar, P. D., in *CRC Handbook of Coastal Processes and Erosion*, CRC Press, USA, 1983.
6. Prasad, K. V. S. R. and Reddy, B. S. R., Proc. 3rd Indian Conference on Ocean Engineering, Indian Institute of Technology, Bombay, 1986.
7. Swaminathan, T. and Sethurathinam, S., Proc. Second National Conference on Dock and Harbour Eng., Chennai, 1987, pp. 292–298.
8. Chandramohan, P., Sanil Kumar, V. and Nayak, B. U., *Indian J. Mar. Sci.*, 1991, **20**, 87–92.
9. Schneider, C., The Littoral Environment Observation (LEO) Data Collection Programme, Coastal Engineering Technical Aid No. 81–5, US Army, Corps of Engineers, CERC, Fort Belvoir, 1981, p. 24.
10. Skovgaard, O., Jonsson, I. G. and Bertelsen, J. A., *J. Waterways, Harbour Coast. Eng. Div.*, 1975, **101**, 15–32.
11. Weishar, L. L. and Byrne, R. J., *Proc. Coastal Eng.*, 1978, 487–506.
12. Galvin, C. J. Jr., Ph D thesis, Massachusetts Institute of Technology, Cambridge, Massachusetts, 1963.

13. Longuet–Higgins, M. S., *J. Geophys. Res.*, 1970, **75**, 6778–6801.
14. Galvin, C. J., Jr., *Coast. Eng.*, 1987, **11**, 115–129.
15. Komar, P. D. and Inman, D. L., *J. Geophys. Res.*, 1970, **75**, 5914–5927.
16. Chandramohan, P., Ph D thesis, Indian Institute of Technology, Madras, 1988, p. 210.
17. Shore Protection Manual, US Army Coastal Engineering Research Centre, Department of the Army Corps of Engineers, Washington, DC, 1984.
18. Miller, H. C., *Coast. Eng.*, 1999, **36**, 301–321.
19. Walton, T. L. Jr. and Bruno, R. O., *J. Coast. Res.*, 1989, **65**, 679–691.
20. Scott, J. R., *J. Ship Res.*, 1965, **9**, 145–152.
21. Nielsen, P., *Coastal Bottom Boundary Layers and Sediment Transport – Advanced Series on Ocean Engineering*, World Scientific, Singapore, 1992, vol. 4, p. 324.
22. Kamphuis, J. W., Proc. 22nd Int. Conf. Coastal Engineering, ASCE, 1990, pp. 2402–2415.
23. Per Bruun, *J. Coast. Res.*, 1997, **13**, 956–958.
24. Chandrasekar, N., Ph D thesis, Department of Industries and Earth Sciences, Tamil University, Thanjavur, 1992.
25. Per Bruun, *Coast Stability*, Danish Engineering Press, Copenhagen, 1954, p. 600.
26. Wang, P. and Kraus, N. C., *J. Waterway, Port, Coast. Ocean Eng.*, 1999, **125**, 118–126.
27. Wang, P., Kraus, N. C. and Davis, R. A. Jr., *J. Coast. Res.*, 1998, **14**, 269–282.
28. Perlin Alexander and Kit Eliezer, *J. Waterway, Port, Coast. Ocean Eng.*, 1999, **125**, 80–87.

ACKNOWLEDGEMENTS. We thank the Director, NIO for permission to use the facilities at the institute. We thank M/s Madras Refineries Limited, Chennai and M/s Dyna Mackowski Power Company, Chennai for funding the wave measurement project. We also thank our colleagues for assistance during field studies. NIO contribution number 3688.

Received 10 September 2001; revised accepted 4 March 2002

Nucleocapsid protein gene sequence studies suggest that soybean bud blight is caused by a strain of groundnut bud necrosis virus

A. I. Bhat[†], R. K. Jain[†,*], A. Varma[†] and S. K. Lal[‡]

[†]Advanced Centre for Plant Virology, Division of Plant Pathology, and [‡]Division of Genetics, Indian Agricultural Research Institute, New Delhi 110 012, India

The nucleocapsid protein (*N*) gene of a tospovirus associated with bud blight-affected soybean plants was cloned and sequenced. The *N* gene was comprised of 831 nucleotides encoding a protein of 276 amino acids. Sequence analyses showed that the gene was most closely related to groundnut bud necrosis virus (GBNV). The amino acid sequence identity with GBNV was 98%, while the identities with other tospoviruses was in the range of 16–84%. On the basis of sequence identity, it is concluded that the soybean tospovirus should be regarded as a strain of GBNV.

TOSPOVIRUSES belonging to the family Bunyaviridae[1] are emerging as serious pathogens affecting the cultivation of many crops in the Indian subcontinent[2,3]. They are quasi-spherical (80–110 nm in diameter) enveloped particles containing three RNA segments, small (S), medium (M) and large (L), and are vectored by thrips in a propagative manner[4]. Tospoviruses have been identified on the basis of amino acid sequence identity of nucleocapsid protein (*N*) gene, host range and vector specificity[5]. On the basis of these parameters, three distinct tospovirus species, groundnut bud necrosis virus (GBNV), groundnut yellow spot virus (GYSV) from groundnut[6–8] and watermelon bud necrosis virus (WBNV) from watermelon[9] have been reported so far from India.

The occurrence of tospovirus infections has also been reported on a large number of legumes, including soybean[10–13]. Recently, association of a tospovirus antigenically related to GBNV with soybean bud blight was established on the basis of biological, serological and nucleic acid hybridization tests[3]. However, the exact identification of the soybean tospovirus remained unaddressed. The virus has seriously affected the soybean cultivation, particularly in Madhya Pradesh[13]. The virus induces necrosis of veins, midrib, petiole, stem and tip or bud. Other symptoms include: yellowing, rugosity, cupping and rolling of leaves. Early-infected plants are severely stunted, with reduced internodal length and many axillary shoots[3,13]. We report here the molecular characterization of soybean tospovirus isolate and discuss whether soybean bud blight is caused by a distinct virus species or a strain of GBNV.

Bud blight-affected soybean samples were collected from an experimental farm at the Indian Agricultural Research Institute (IARI), New Delhi. The virus was maintained and propagated on cowpea (*Vigna unguiculata* cv. Pusa Komal) in a glasshouse through mechanical inoculations using 0.1 M phosphate buffer, pH 7.2, containing 0.1% 2-mercaptoethanol.

Total RNA extracted from healthy and infected cowpea tissue using RNesay kit (Qiagen Inc., Chatsworth, CA, USA) was used as a template for reverse transcription polymerase chain reaction (RT–PCR). RT–PCR was based on the procedure described earlier[14]. The primer pair derived from the *N* gene sequence of GBNV[7] and watermelon silver mottle virus (WSMV)[15] was used to prime the amplification. The genome sense

*For correspondence. (e-mail: rkjain@bic-iari.ren.nic.in)